CrossMark

REGULAR ARTICLE

Spatial variation of soil respiration is linked to the forest structure and soil parameters in an old-growth mixed broadleaved-Korean pine forest in northeastern China

Baoku Shi · Weifeng Gao · Huiying Cai · Guangze Jin

Abstract

Aims The aim of this study was to quantify and understand the driving factors of the spatial variation of soil respiration (R_S) in an old-growth mixed broadleaved-Korean pine forest in northeastern China.

Methods All woody stems ≥1 cm diameter at breast height (DBH) were measured in the 9 ha plot. Simultaneous measurements of R_S, soil temperature (T_S) and soil water content (W_S) were conducted for 256 sampling points on a regular 20-m grid refined with 512 additional sampling points randomly placed within each of the 20-m blocks in May, July and September of 2014.

Results The variogram analyses revealed 87–91 % of the sample variance was explained by autocorrelation over a range of 15 to 23 m during the observation periods. The R_S were highly correlated among the measurements made in May, July and September. The model indicated that the W_S, bulk density (BD) and maximum DBH for trees within 3 m (radius) of the measurement collars explained 46 % of the spatial variation in R_S seasonally averaged across three observations.

Conclusions The spatial patterns of R_S remained constant across the three measurement campaigns. The spatial variation in R_S was primarily controlled by the W_S and forest stand structure.

Keywords Old-growth forest · CO_2 efflux · Spatial variation · Tree diameter · Ecosystem carbon cycling · Geostatistics

B. Shi · W. Gao · H. Cai · G. Jin (✉)
Center for Ecological Research, Northeast Forestry University, Harbin 150040, China
e-mail: taxus@126.com

B. Shi
Forest Survey and Design Institute of Jilin Province, Changchun 130022, China

Introduction

Forest ecosystems are major terrestrial carbon (C) sinks that sequester large amounts of atmospheric CO_2 and offer the potential for the mitigation of climate change (Lorenz and Lal 2010). The C balance of old growth forests has traditionally received little attention because they are believed to be C neutral (Odum 1969). However, recent study reported that old growth forests act as net sinks of atmospheric CO_2 (Luyssaert et al. 2008; Hudiburg et al. 2009; Lewis et al. 2009). The quantification of the major components of forest ecosystem C cycling and the understanding of their control factors are prerequisites for the estimation of C sources or sinks. Soil respiration (R_S) is the second largest C flux in the forest ecosystem after gross primary production and thus plays a crucial role in ecosystem C cycling (Davidson et al. 2006).

R_S originates from rhizospheric respiration (respiration from live roots and their associated mycorrhizal

fungi and rhizosphere microorganisms) and heterotrophic respiration (respiration from microorganisms decomposing litter and soil organic matter), two components involving various biological and ecological processes and responding differently to environmental changes (Scott-Denton et al. 2006; Song et al. 2015). Therefore, there is substantial temporal and spatial variation in R_S. The temporal variation of R_S is straightforward to capture by using continuous automated measurements and is known to be affected by the soil temperature (T_S) and soil water content (W_S) (Wang et al. 2013). In contrast, the spatial variation of R_S remains under-researched, which is mostly uncertain due to the limited measurement methods and the high labour and time costs (Dore et al. 2014; Prolingheuer et al. 2014). Geostatistics is an appropriate methodology for the capture, representation and interpretation of the spatial patterns of R_S and the soil properties and has been applied over the last few decades (Robertson and Gross 1994; Teixeira et al. 2013; Yuan et al. 2013; Ferré et al. 2015).

In addition to the quantification of spatial variation in R_S, identifying key factors that regulate the spatial variation in R_S is essential for designing an optimal sampling approach and accurately estimating R_S at the ecosystem scale. Biotic factors, such as the stand structure, fine root biomass and leaf litterfall, all contribute to the spatial variation of R_S at the ecosystem scale (Katayama et al. 2009; Barba et al. 2013). Trees are involved directly in root respiration and indirectly in root-derived rhizosphere respiration and the decomposition of aboveground and belowground litter by microorganisms (Bréchet et al. 2011). Therefore, the tree diameter may be a good proxy for the biotic factors that would explain the spatial variation of R_S (Bréchet et al. 2011; Luan et al. 2012). The main abiotic factors influencing the identified spatial variation of R_S are the soil water content, which controls gas diffusivity (CO_2 and O_2) and microbial activity (Herbst et al. 2009; Martin and Bolstad 2009; Yoon et al. 2014), and the soil substrate quantity and quality, such as the soil organic carbon content (SOC), soil total nitrogen content (TN) and soil C:N ratio (Luan et al. 2012; Ngao et al. 2012). Nonetheless, the contribution of these factors is highly variable in different ecosystems and needs to be verified.

The Asian temperate mixed forest is predominantly found in northeastern China (40°15′–50°20′N and 126°–135°30′E) and is one of the three largest areas of temperate mixed forest in the world (i.e., northeastern North America, Europe, and Eastern Asia) (Wang et al. 2006). The temperate forest in northeastern China accounts for approximately one-third of the forested land area and forest stock in China (State Forestry Administration (SFA) 2005). The primary mixed broadleaved-Korean pine (*Pinus koraiensis*) forest is the zonal climax vegetation in northeast China. Previous studies by our laboratory and other researchers have reported the seasonal dynamic of R_S and its components in this forest (Wang et al. 2010; Shi et al. 2015). However, thus far, no studies have been conducted in this important forest to elucidate the mechanisms and quantification of the spatial variation of R_S, which are critical for estimating the C budgets on the scales of the ecosystems to the regional scale. Our study attempts to fill in this gap of knowledge, and our specific objectives were to (1) quantify and visualize the spatial variation of R_S and its temporal changes in an old-growth temperate mixed forest in northeastern China and (2) identify the roles of biotic and abiotic factors, such as the forest structure (size and spatial distribution of the trees), T_S, W_S, bulk density (BD), SOC, TN, soil C:N ratio and soil pH, that are used to determine the spatial variation in R_S at the ecosystem scale. We hypothesized that (1) the spatial variation of R_S remained constant during the growing season and (2) the spatial variation of R_S would mainly be determined by the W_S, BD and the spatial distribution of the tree size.

Materials and methods

Study sites and experimental design

The study site was in the Liangshui National Reserve (47°10′50″N, 128°53′20″E) in northeastern China. The region lies on the eastern part of Eurasia, and the climate is classified as continental monsoon. The mean annual temperature is −0.3 °C, with a frost-free period of 100 to 120 days and snow period of 130 to 150 days. The daily air temperature revealed distinct seasonal variations throughout the growing season (Shi et al. 2015). The mean annual precipitation is 676 mm. The soil is dark-brown forest soil by the Chinese soil classification,

which is equivalent to Humaquepts or Cryoboralfs based on the American Soil Taxonomy (Soil Survey Staff 1999). The total area of the reserve is 12,133 ha, with 1.88 million m^3 of growing stock and an average canopy cover of 98 %. The mixed broadleaved-Korean pine forest accounts for 63.7 % and 77.4 % of the forested area and standing tree volume in the whole reserve, respectively, which has not been disturbed for more than 300 years. The forest is primarily composed of *Pinus koraiensis*, *Betula costata*, *Tilia amurensis*, *Acer ukurunduense*, *Abies nephrolepis*, *Ulmus laciniata*, *Acer tegmentosum*, *Fraxinus mandshurica*, and *Acer mono*.

The 9-ha (300 × 300 m) survey plot was established in the mixed broadleaved-Korean pine forest in 2005 (Fig. 1). A 20 × 20 m square grid was placed within the plot, and 256 intersections were considered to be R_S measurement base points. To capture the spatial variation in the R_S at a finer scale, two additional sample points (2, 5, or 8 m) were selected in a randomly assigned cardinal direction (N, NE, E, SE, S, SW, W or NW) from the base point (Webster and Oliver 2007). Thus, we selected a total of 768 sample locations in the 9-ha plot (Fig. 2).

Soil respiration and soil climate

R_S was measured using an LI-6400 portable CO_2 infrared gas analyser (IRGA) (LI-COR Inc., Lincoln, NE, USA) in spring (May), summer (July) and autumn

(September) of 2014 (one measurement in each season). No measurements were conducted in winter because the analysers cannot run at low temperatures. Each measurement campaign lasted for about one week and was performed from 10:00 am to 16:00 pm. To reduce the time required for each measurement campaign, two LI-6400 analysers (IRGA) carried out the field work simultaneously. R_S was measured on rainless days, and when a rain event occurred, the measurements were interrupted and resumed the next day to reduce the effect of rainfall on R_S. PVC collars (10.4-cm diameter × 6 cm height) were installed at each sampling point at the beginning of May, which was one week before the first measurement campaign. The collars were inserted 4 cm into the soil (including the litter layer). Simultaneous with each R_S measurement, the T_S was measured at a depth of 5 cm using a thermocouple penetration probe (Li-6000-09 TC, LI-COR, Inc.). The W_S at 0–10 cm soil depth was measured using a time-domain reflectometry (TDR) probe (IMKO, Ettlingen, Germany) at two points next to each collar.

Stand structural parameters and soil properties

In July 2010, the diameter at breast height (DBH) of each tree with a DBH greater than 1 cm was measured, as well as its position in the 9-ha plot (Fig. 2). Based on these data, we calculated a series of stand structural parameters, including the total basal area (BA), maximum DBH (max. DBH) of the trees, and mean DBH of
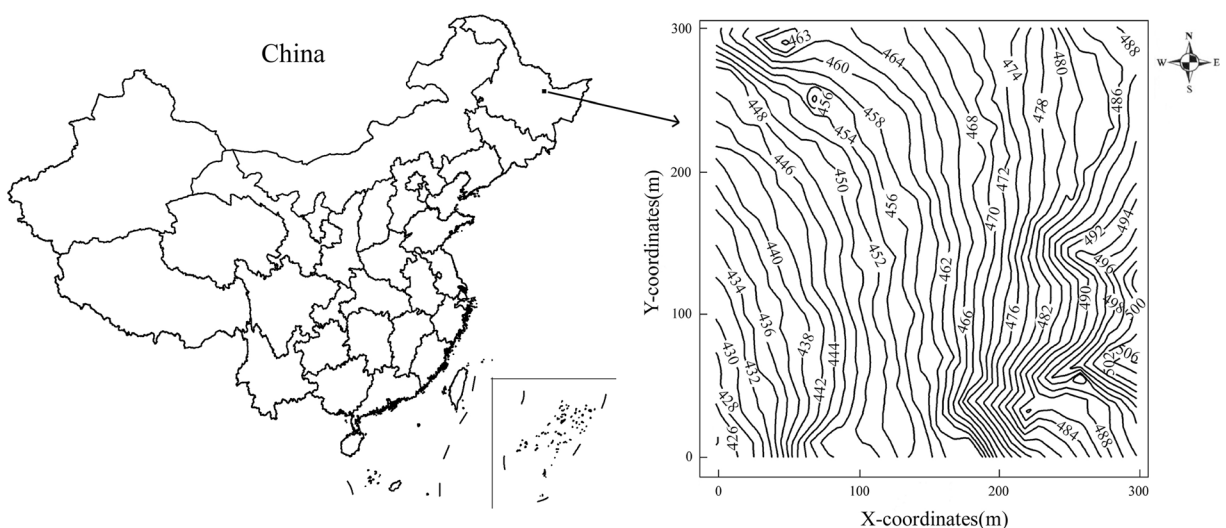
Fig. 1 The location and contour map (elevation unit is in m) of the 9-ha (300 × 300 m) Liangshui temperate forest plot

Fig. 2 Positions of all of the living trees (*open circles*, symbol sizes indicate the diameter at breast height of the trees and the depicted diameters are enlarged for comparison) and the soil respiration sampling design (*filled red circles*) within a 9-ha plot
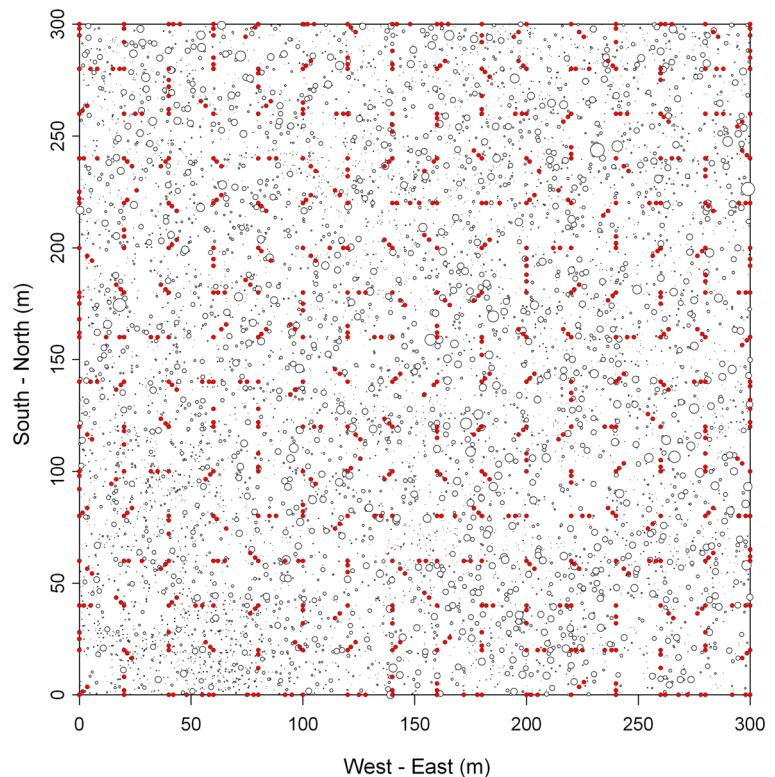
the trees within 1–10 m of each R_S measurement point. One soil sample was collected from the top of the soil near each R_S measurement base point using 100-ml (50.46-mm diameter, 50-mm height) cylinders to analyse the BD. In July 2013, three soil subsamples were collected using a soil corer (5-cm diameter) at 0–10 cm of soil approximately 0.5 m from each sample location (collar). These three subsamples were mixed as one sample to analyse the soil nutrients, including the SOC and TN. The SOC was determined by a multi N/C 2100 analyser (Analytik Jena AG, Jena, Germany). The TN was measured using a Hanon K9840 auto Kjeldahl analyser (Jinan Hanon Instruments Co., Ltd., China). The SOC and TN were also used to calculate the C:N ratio. The soil pH was measured in water (1: 2.5 w/v).

Statistical analysis

Geostatistical analyses (variogram calculation, semivariogram model fitting and kriging) were performed with GS+ version 7.0 for Windows (Gamma Design Software 2004). Before the geostatistical analysis, the data were logarithmically transformed to normalise skewed frequency distributions. The experimental

semivariance $\gamma (h)$ for the distance interval h was calculated as follows:

$$\gamma(h) = \frac{1}{2n(h)} \sum_{i=1}^{n} \left[z(x_i) - z(x_i + h)\right]^2 \quad (1)$$

where $n(h)$ is the number of observation pairs separated by the distance h and $z(x_i)$ and $z(x_i + h)$ are the variable values at the locations x_i and $x_i + h$. An exponential variogram was used to model the experimental variograms obtained.

$$\gamma(h) = c_0 + c\left(1 - e^{-h/a}\right) \quad (2)$$

where c_0 is the nugget, $c_0 + c$ is the sill, and a is the correlation length. The practical range for the exponential model is $3a$. In the following, the proportion of the model sample variance ($c_0 + c$) explained by the structural variance (c) was used as a normalized measure of spatial dependence (Robertson et al. 1993). The experimental variogram was calculated using an active lag distance of 212.13 m (slightly less than half of the maximum separation distance between the sampling points) and a lag class distance of 14.14 m.

To construct the interpolation maps, we used ordinary block kriging with a block size of 3.23 m across the field and a 2×2 discretization grid within each block. The block kriging and the exponential semivariance models were used for mapping the spatial patterns of the R_S and W_S. According to previous studies (Herbst et al. 2009) and our hypothesis, the relationship between R_S and the W_S could be closer when compared to the T_S, thus, the map was not created for the T_S. The maps were produced using Surfer spatial analysis software (Version 11, Golden Software, Inc., CO, USA).

The regression analyses were used to examine the similarities in the spatial patterns of the R_S among the measurement campaigns. The relationships between the R_S and the soil climate, the stand structural parameters and the soil properties were also examined by linear regression (Pearson correlation coefficient). A backward multiple regression analysis was carried out on the selected variables that could control the spatial variation of the R_S during the observation periods. Logarithmic transformation of R_S was performed as needed to achieve linearity and homoscedasticity. The raw data supporting the paper's main results are available as electronic supplementary material, in an MS Excel file. These statistical analyses were performed using SPSS 18.0 software (SPSS Inc., Chicago, USA). The scatter and line graphs were generated using Sigmaplot 12.5 software (Systat Software, Inc., San Jose, CA, USA).

Results

Spatial variation of soil respiration

The seasonal pattern of the spatial mean R_S was similar to that of T_S, peaking in summer (Table 1). The spatial coefficient of variance (CV) of T_S was lower (7–19 %) than that of R_S (42–55 %) during the observation periods. In contrast, the CV for W_S was between 32 and 34 %, which was higher than that of T_S. Kriged maps were used to provide a visual impression of the spatial patterns of R_S and W_S (Fig. 3). W_S was relatively high in the north and the west of the plot during the observation periods, whereas R_S was low at these points. The areas of lower R_S in the spring remained low during the summer and autumn and did not vary with the season.

We found a significantly positive correlation between the R_S in spring and summer ($r = 0.711$, $P < 0.01$), summer and autumn ($r = 0.738$, $P < 0.01$) and spring and autumn ($r = 0.604$, $P < 0.01$).

The proportion of the structural variance (c) to the sill ($c_0 + c$) and the spatial autocorrelation ranges for R_S differed little between the sampling periods, ranging between 87 and 91 % and between 15 and 23 m, respectively (Table 2, and Fig. 4). The proportion and autocorrelation ranges for T_S differed substantially between the sampling periods. The proportion for T_S was higher in summer (89 %) and in autumn (88 %) than in spring (52 %), whereas the autocorrelation ranges were lower in summer (27 m) than in spring (285 m) and autumn (508 m). The proportion for W_S was lower in autumn (69 %) than in spring (90 %) and summer (91 %), and the autocorrelation ranges varied from 17 m (spring) to 67 m (autumn). The autocorrelation range for the T_S-average (105 m) was higher than for the R_S-average (18 m) and the W_S-average (42 m).

Factors affecting the spatial variation of soil respiration

The spatial variation of R_S was positively related to T_S and was negatively correlated with W_S and BD during the observation periods ($P < 0.05$, Table 3). We found significant correlations in the relationships between R_S and the forest structural parameters (mean DBH, BA and max. DBH, $P < 0.05$), and the correlations depended on the distance from the measurement locations (Table 3, and Fig. 5). The correlations between the mean DBH_1, BA_4, max. DBH_3 and R_S were strongest during the observation periods, and they were introduced for backward multiple regression analysis (Table 3, and Fig. 5). With the spatial variation of R_S, the SOC had a weak significant correlation in all of the observation periods except for spring ($P < 0.05$), whereas the pH had a significant correlation in all of the observation periods except for autumn ($P < 0.001$). No significant correlation of the R_S with the TN and C:N was found ($P > 0.05$, Table 3). Subsequently, all of the correlated variables that showed significant relationships with R_S were used in a backward multiple regression analysis (Table 3, Table 4). The model indicated that the W_S-average, BD and max. DBH_3 explained 46 % of the spatial variation in the R_S-average. The regression model in summer showed an R^2 of 0.45, which was higher than for spring (0.27) and autumn (0.36).

Table 1 Descriptive statistics for the soil respiration, soil climate, stand structural parameters and soil properties

Parameter[a]	Mean	Maximum	Minimum	SD	CV	N
R_S-spring (μmol CO_2 m^{-2} s^{-1})	2.02	5.08	0.39	0.86	0.42	768
R_S-summer (μmol CO_2 m^{-2} s^{-1})	4.19	13.31	0.10	2.29	0.55	768
R_S-autumn (μmol CO_2 m^{-2} s^{-1})	3.57	10.58	0.38	1.82	0.51	768
R_S-average (μmol CO_2 m^{-2} s^{-1})	3.26	9.66	0.57	1.50	0.46	768
T_S-spring (°C)	6.65	11.13	2.28	1.25	0.19	768
T_S-summer (°C)	15.35	18.37	8.09	1.19	0.08	768
T_S-autumn (°C)	13.87	17.86	10.50	0.99	0.07	768
T_S-average (°C)	11.96	14.00	8.15	0.73	0.06	768
W_S-spring (%)	29.01	65.64	3.44	9.40	0.32	768
W_S-summer (%)	30.43	65.91	3.26	10.09	0.33	768
W_S-autumn (%)	30.02	66.43	5.14	10.31	0.34	768
W_S-average (%)	29.82	65.99	7.82	8.95	0.30	768
Mean DBH$_1$ (cm)	7.86	78.30	1.00	12.15	1.55	287
BA$_4$ (m^2/ha)	43.62	230.83	0.08	43.04	0.99	586
Max DBH$_3$ (cm)	26.64	86.00	1.00	21.13	0.79	578
SOC (g/kg)	74.96	247.50	5.84	46.65	0.62	767
TN (g/kg)	8.30	19.91	1.27	3.29	0.40	767
C:N	9.42	77.18	0.65	6.29	0.67	767
pH	5.77	7.14	4.45	0.38	0.07	767
BD (g/m^3)	0.63	1.76	0.12	0.26	0.41	256

[a] R_S Soil respiration; T_S Soil temperature at depths of 0–5 cm; W_S Soil water content at depths of 0–10 cm; Mean DBH$_1$ mean DBH for trees within 1 m (radius) of the measurement collars; BA$_4$ Total basal area for trees within 4 m (radius) of the measurement collars; Max DBH$_3$ Maximum DBH for trees within 3 m (radius) of the measurement collars; SOC Soil organic carbon at depths of 0–10 cm; TN Total nitrogen content at depths of 0–10 cm; BD Bulk density at depths of 0–10 cm
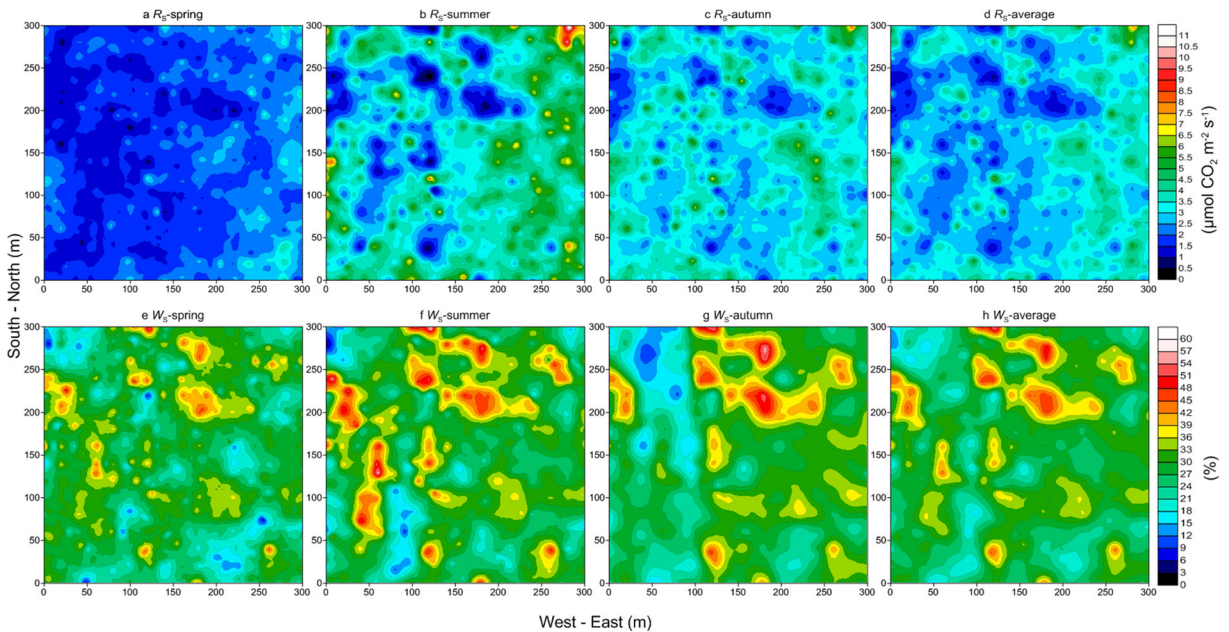
Fig. 3 Spatial distribution of soil respiration (R_S) and the soil water content (W_S) in spring, summer, autumn and the growing season

Table 2 Summary of the semivariogram model parameters for soil respiration and the soil properties

	Model	Nugget c_0	Sill $c_0 + c$	Proportion $c/(c_0 + c)$	Range (m)	R^2	Residual SS
R_S-spring [a]	Exponential	0.0140	0.1600	0.913	17.1	0.481	1.95×10^{-3}
R_S-summer	Exponential	0.0550	0.4280	0.871	22.5	0.830	4.26×10^{-3}
R_S-autumn	Exponential	0.0324	0.2648	0.878	14.7	0.953	1.74×10^{-4}
R_S-average	Exponential	0.0259	0.2308	0.888	18.0	0.850	7.60×10^{-4}
T_S-spring	Exponential	0.0214	0.0445	0.520	285.3	0.945	2.85×10^{-5}
T_S-summer	Exponential	0.0008	0.0071	0.887	27.3	0.877	1.25×10^{-6}
T_S-autumn	Exponential	0.0009	0.0070	0.875	508.2	0.974	6.17×10^{-7}
T_S-average	Exponential	0.0017	0.0043	0.601	105.0	0.925	4.18×10^{-7}
W_S-spring	Exponential	0.0139	0.1388	0.900	16.8	0.776	3.76×10^{-4}
W_S-summer	Exponential	0.0106	0.1182	0.910	31.5	0.893	3.44×10^{-4}
W_S-autumn	Exponential	0.0434	0.1408	0.692	67.2	0.954	2.64×10^{-4}
W_S-average	Exponential	0.0242	0.0910	0.734	42.3	0.953	8.16×10^{-5}
SOC	Exponential	0.2082	0.4174	0.501	148.8	0.955	1.86×10^{-3}
TN	Exponential	0.0240	0.2040	0.882	20.4	0.773	1.14×10^{-3}
C:N	Exponential	0.1286	0.2712	0.526	216.0	0.980	4.09×10^{-4}
pH	Exponential	0.0004	0.0042	0.917	15.9	0.702	4.88×10^{-7}

[a] R_S Soil respiration (μmol CO_2 m^{-2} s^{-1}); T_S Soil temperature at depths of 0–5 cm (°C); W_S Soil water content at depths of 0–10 cm (%); SOC Soil organic carbon at depths of 0–10 cm (g/kg); TN Total nitrogen content at depths of 0–10 cm (g/kg)

## Discussion

Spatial variation of soil respiration

Our estimated CV of R_S, T_S and W_S correspond well with the CV of temperate forests in previous studies. Ngao et al. (2012) reported that the spatial CV of R_S varied throughout the measurement period, ranging from 9 to 62 % in a temperate beech forest. A strong spatial heterogeneity of R_S was observed in the regenerated temperate forest, with coefficients of variance of 25 to 40 % (Luan et al. 2012). Consistent with the previous findings (Ngao et al. 2012; Dore et al. 2014), we found that the CV of T_S (7–8 %) was much lower than the CV of R_S (51–55 %) and W_S (33–34 %) in summer and autumn (Table 1). These findings indicated that the T_S was not an important variable for explaining the spatial variation of R_S in summer and autumn. Moreover, Wang et al. (2006) reported that the CV of R_S within the plots (20 × 30 m) varied from 20 to 27 % for four secondary forests and two plantations in northeastern China, which were lower than those reported in our study. A study by Wang et al. (2006) and our study have adjacent geographical positions, the same original vegetation in the history, climate and soil types. As such, the differences

in the CV of R_S between the two studies may be attributed to the fact that the stand structure of the primary forest in our study was more complex in contrast to the secondary forests and plantations studied by Wang et al. (2006), and the plot spatial extent was larger in contrast to that of the latter.

The autocorrelation range of R_S depended on the plot spatial extent and the distance between the samples (Western and Blöschl 1999; Prolingheuer et al. 2014). In this study, R_S shows a pronounced spatial autocorrelation, and 87–91 % of the sample variance was explained by an autocorrelation over a range of 15 to 23 m (Table 2, and Fig. 4). The range for the R_S of a 72 × 72 m plot in a broad-leaved mixed temperate forest was smaller than 6 m, which could be explained by the smaller spatial extent than in this study (Søe and Buchmann 2005). However, our results should be interpreted with caution, as geostatistics involves uncertainties and subjective decisions for estimating the semivariance (Webster and Oliver 2007).

Sources of soil respiration variation

Kriged maps of R_S and the significant correlations among the R_S of the three measurement campaigns
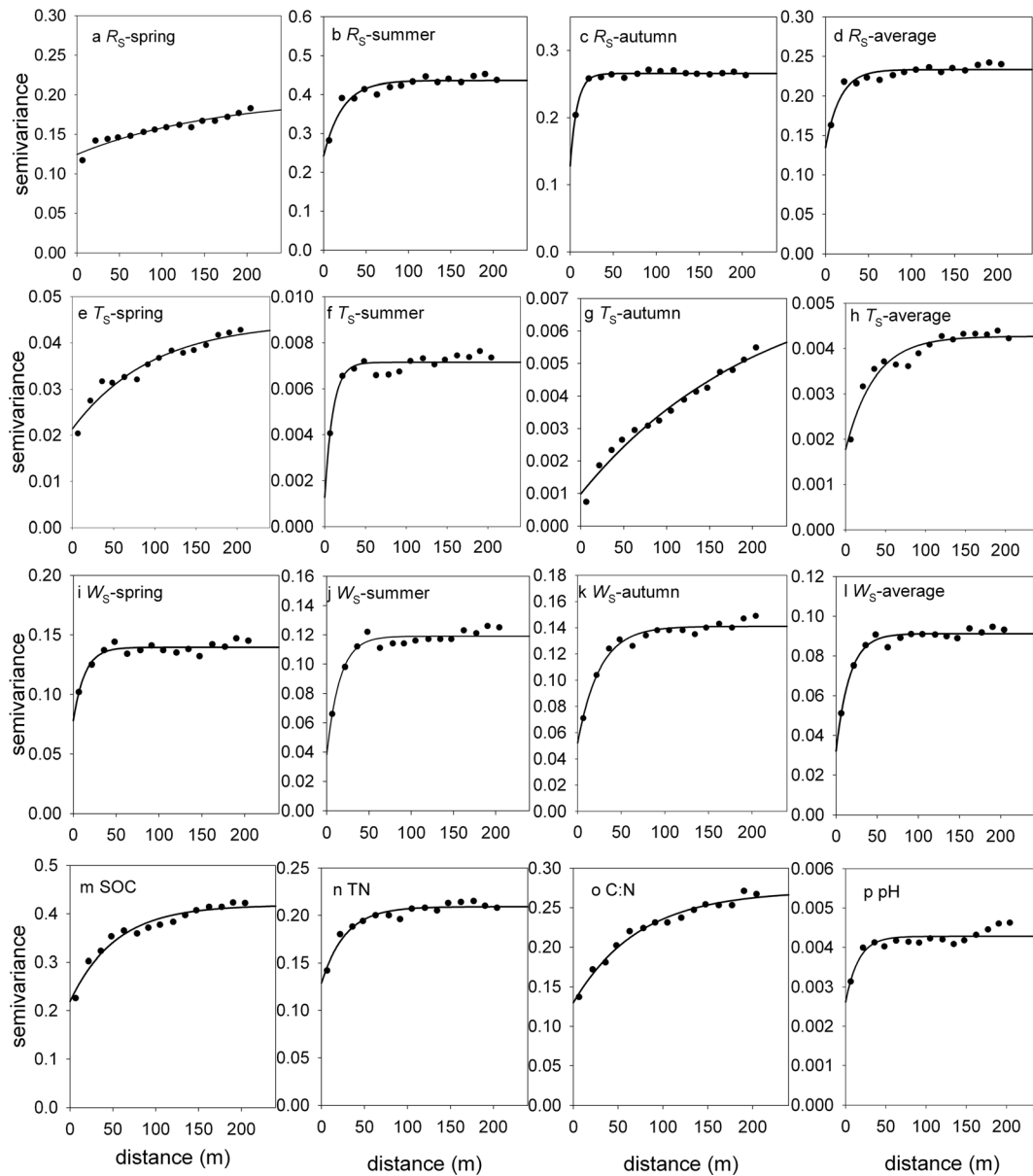
Fig. 4 Semivariograms of soil respiration and the soil properties. R_S: soil respiration; T_S: soil temperature at depths of 0–5 cm; W_S: soil water content at depths of 0–10 cm; SOC: soil organic carbon at depths of 0–10 cm; TN: total nitrogen content at depths of 0–10 cm

confirmed the hypothesis that the spatial patterns of R_S remained constant across the three measurement campaigns. Our result is consistent with other studies (Søe and Buchmann 2005; Martin and Bolstad 2009; Luan et al. 2012). As reported in six northern hardwood sites and two aspen sites (Martin and Bolstad 2009), the pattern of a consistently high or consistently low R_S over time indicates the existence of a mechanism or mechanisms that consistently produce more or less CO_2 in the soil profile. The above reasoning was also

supported by the results inferred from our final multiple linear regressions (Table 4). The regression model suggested that the spatial variation in R_S was mainly controlled by the W_S, BD and max. DBH$_3$, which were relatively stable. However, T_S was also an important determinate of the spatial variation of R_S in spring, which may be attributed to the fact that R_S was limited by the low soil temperature and that the CV of T_S in spring (19 %) was higher than those (7–8 %) in summer and autumn. The effects of the W_S on the spatial

Table 3 Correlation coefficients between soil respiration and the soil climate, stand structural parameters and soil properties

	T_S- spring	T_S- summer	T_S- autumn	T_S- average	W_S- spring	W_S- summer	W_S- autumn	W_S- average	Mean DBH$_1$	BA$_4$	Max. DBH$_3$	SOC	TN	C:N	pH	BD
R_S- spring [a]	0.29**				-0.34**				0.14*	0.27**	0.29**	-0.01	0.04	-0.03	0.18**	-0.17*
R_S- summer		0.28**				-0.53**			0.19*	0.36**	0.32*	0.07*	-0.01	0.04	0.16**	-0.15*
R_S- autumn			0.13**				-0.41**		0.25**	0.37**	0.38**	0.11*	0.07	0.03	0.07	-0.15*
R_S- average				0.20**				-0.53**	0.23**	0.39**	0.38**	0.08*	0.03	0.03	0.15**	-0.16*

a R_S Soil respiration (μmol CO$_2$ m^{-2} s^{-1}); T_S Soil temperature at depths of 0–5 cm (°C); W_S Soil water content at depths of 0–10 cm (%); BA$_4$ Total basal area for trees within 4 m (radius) of the measurement collars (cm); Mean DBH$_1$ mean DBH for trees within 1 m (radius) of the measurement collars (cm); Max DBH$_3$ maximum DBH for trees within 3 m (radius) of the measurement collars (m); SOC Soil organic carbon at depths of 0–10 cm (g/kg); TN Total nitrogen content at depths of 0–10 cm (g/kg); BD Bulk density at depths of 0–10 cm (g/m^3)

* $P < 0.05$

** $P < 0.001$ and $P > 0.05$ otherwise

variation in R_S can be direct or indirect and involve physical or biological mechanisms. The relationship between R_S and W_S usually shows a threshold value (approximately 20 %; Xu and Qi 2001; Herbst et al. 2009; Moyano et al. 2013; Cartwright and Hui 2015). Below this threshold, a positive linear relationship between R_S and W_S was found (Xu and Qi 2001; Chang et al. 2014; Escolar et al. 2015), and this is due to the low W_S that causes a decrease in the rate of diffusion of soluble substrates, which can limit soil microbial respiration (Davidson et al. 2006). Above the threshold, R_S is negatively correlated with W_S (Xu and Qi 2001; Cartwright and Hui 2015). The reason for this is that a high W_S not only reduces CO_2 transport but can also limit O_2 availability and microbial activity (Smith et al. 2003). However, our study did not find a threshold value. It is possible that the R_S measurement points (W_S-average > 20 %) account for 90 % of the total due the fact that our site had plenty of rainfall in the growing season and that the water holding capacity of the soil was high. Thus, W_S was always relatively high at our study site, and it was never low enough to limit R_S.

The C assimilated by a tree is transported to the roots and is used to support the roots and the associated mycorrhizal fungi and rhizosphere microorganism respiration, which further affects the total soil respiration because root respiration accounts for approximately 50 % of the total (Bond-Lamberty et al. 2004; Kuzyakov and Gavrichkova 2010). Thus, the spatial distribution of tree size may explain the spatial variation of R_S. The significant correlations between R_S and the forest structural parameters were found in previous studies (Søe and Buchmann 2005; Katayama et al. 2009; Luan et al. 2012). Katayama et al. (2009) reported that the mean DBH within 6 m of the measurement points had a significant linear relationship with R_S in a Bornean tropical rainforest ($R^2 = 0.60$). Luan et al. (2012) also found that the stand structure parameters (including the BA, max. DBH and mean DBH) within 4–5 m of the measurement points had a significant influence on the spatial variation of R_S in a regenerated temperate forest. Our results showed that the mean DBH$_1$, BA$_4$ and max. DBH$_3$ were significantly correlated to the spatial variation of R_S. This confirms the assumption that the forest stand structure determines the spatial variation in R_S. Furthermore, the final model indicated that the max. DBH$_3$ was one of the three most important parameters for explaining the spatial variation of the R_S-average. This result suggested that the largest

Fig. 5 Changes in the correlations between soil respiration (R_S) and the maximum DBH (max. DBH), basal area (BA), and mean DBH with distance (from 1 m to 10 m) from each measurement point in spring, summer, autumn and the growing season
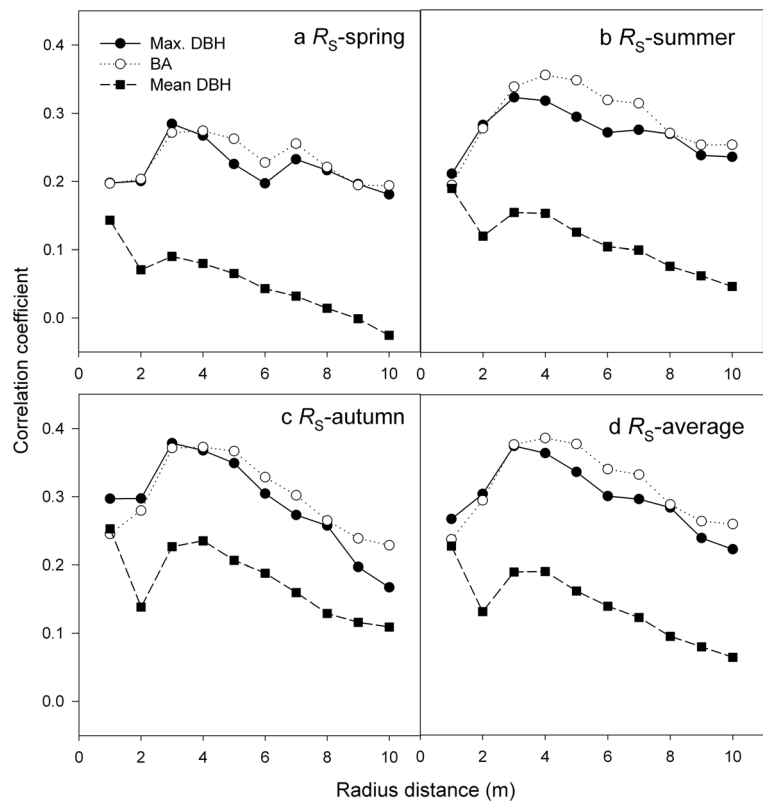
trees may influence the local spatial variation of R_S, which may be attributed to the fact that large trees may have a greater belowground C allocation than small trees or that the spatial distribution of emergent trees may affect the root distribution of surrounding smaller trees, resulting in the spatial variation of R_S (Søe and Buchmann 2005; Bréchet et al. 2011; Luan et al. 2012; Ohashi et al. 2015).

Despite the promising results from the model fits discussed above, there was considerable variation (54 %) in the spatial heterogeneity of R_S that could not be explained. Several other ecologically driven processes and potential biases could contribute to unexplained variation. First, there was a significant, but weak correlation between R_S and the SOC during all of the observation periods, except for spring. The light fraction organic carbon may explain the spatial variation of R_S better when compared to the SOC, as it can partly reflect the substrate availability or the microbial activity (Laik et al. 2009; Luan et al. 2012). Future studies are needed to confirm this inference. Second, the stand structure and R_S were not investigated simultaneously, which may be a potential bias. However, this old-growth forest has not been recently disturbed and

the stand structure was relatively stable. Thus, it was appropriate to estimate the relationship between the stand structure parameters and R_S in this study, even though the two variables were investigated in the different year. Finally, the relationship between R_S and the root biomass and soil microbial biomass may be close. However, obtaining these driving factors is difficult due to high labour and time costs. Our results showed that the forest stand structure contributed to the spatial variation of R_S at the ecosystem scale. This is an important finding to extrapolate R_S spatially using forest stand structural parameters at the ecosystem scale where the tree diameter are more easily obtained than root mass (Katayama et al. 2009).

Conclusion

Our results demonstrated that R_S had a strong spatial heterogeneity and spatial autocorrelation. These results have implications for an optimum sampling setup. For example, at a plot or ecosystem scale, it is possible to generate biased average R_S estimates if the number of

Table 4 Regression models for spatial variation in soil respiration and the soil climate, stand structural parameters and soil properties

	RS-spring		RS-summer		RS-autumn		RS-average	
	Parameters[a],*	Beta	Parameters	Beta	Parameters	Beta	Parameters	Beta
	W_S-spring	−0.324	W_S-summer	−0.623	W_S-autumn	−0.481	W_S-average	−0.592
	T_S-spring	0.237	BD	−0.243	Max. DBH$_3$	0.246	BD	−0.274
	BD	−0.205	Max. DBH$_3$	0.131	BD	−0.241	Max. DBH$_3$	0.176
	Max. DBH$_3$	0.173						
	$\ln R_S = 0.629 - 0.014W_S + 0.078T_S - 0.331BD + 0.003$Max. DBH$_3$		$\ln R_S = 2.772 - 0.04W_S - 0.623BD + 0.004$Max. DBH$_3$		$\ln R_S = 2.012 - 0.024W_S + 0.006$Max. DBH$_3 - 0.486BD$		$\ln R_S = 2.247 - 0.032W_S - 0.519BD + 0.004$Max. DBH$_3$	
	$R^2 = 0.27$		$R^2 = 0.45$		$R^2 = 0.36$		$R^2 = 0.46$	

[a] R_S Soil respiration (μmol CO_2 m^{-2} s^{-1}); T_S Soil temperature at depths of 0–5 cm (°C); W_S Soil water content at depths of 0–10 cm (%); Max DBH$_3$ Maximum DBH for trees within 3 m (radius) of the measurement collars (cm); BD Bulk density at depths of 0–10 cm (g/m^3)

* All models $P < 0.001$

replicates is small (<the number of measurements required to obtain an average R_S within 20 % of its actual value at the 95 % confidence level) or measurement points are located close to each other (<spatial autocorrelation length). Additionally, the spatial patterns of R_S did not remarkably vary from season to season. The spatial variation of R_S was tightly linked to the forest stand structure and soil parameters, such as the W_S and BD, which were easily obtained. These findings enable us to understand the mechanisms underlying R_S and estimate the net ecosystem C exchange at the ecosystem scale in an old-growth mixed broadleaved-Korean pine forest in northeastern China.

References

Barba J, Yuste JC, Martínez-Vilalta J, Lloret F (2013) Drought-induced tree species replacement is reflected in the spatial variability of soil respiration in a mixed Mediterranean forest. For Ecol Manag 306:79–87

Bond-Lamberty B, Wang CK, Gower ST (2004) A global relationship between the heterotrophic and autotrophic components of soil respiration? Glob Chang Biol 10(10):1756–1766

Bréchet L, Ponton S, Alméras T, Bonal D, Epron D (2011) Does spatial distribution of tree size account for spatial variation in soil respiration in a tropical forest? Plant Soil 347:293–303

Cartwright J, Hui DF (2015) Soil respiration patterns and controls in limestone cedar glades. Plant Soil 389:157–169

Chang CT, Sabaté S, Sperlich D, Poblador S, Sabater F, Gracia C (2014) Does soil moisture overrule temperature dependency of soil respiration in mediterranean riparian forests? Biogeosci Discuss 11:7991–8022

Davidson EA, Janssens IA, Luo YQ (2006) On the variability of respiration in terrestrial ecosystems: moving beyond Q_{10}. Glob Chang Biol 12:54–164

Dore S, Fry DL, Stephens SL (2014) Spatial heterogeneity of soil CO_2 efflux after harvest and prescribed fire in a California mixed conifer forest. For Ecol Manag 319:150–160

Escolar C, Maestre FT, Rey A (2015) Biocrusts modulate warming and rainfall exclusion effects on soil respiration in a semi-arid grassland. Soil Biol Biochem 80:9–17

Ferré C, Castrignanò A, Comolli R (2015) Assessment of multi-scale soil-plant interactions in a poplar plantation using

geostatistical data fusion techniques: relationships to soil respiration. Plant Soil 390:95–109

Herbst M, Prolingheuer N, Graf A, Huisman JA, Weihermüller L, Vanderborght J (2009) Characterisation and understanding of bare soil respiration spatial variability at plot scale. Vadose Zone J 8:762–771

Hudiburg T, Law B, Turner DP, Campbell J, Donato D, Duane M (2009) Carbon dynamics of Oregon and northern California forests and potential land-based carbon storage. Ecol Appl 19:163–180

Katayama A, Kume T, Komatsu H, Ohashi M, Nakagawa M, Yamashita M, Otsuki K, Kumagai T (2009) Effect of forest structure on the spatial variation in soil respiration in a Bornean tropical rainforest. Agric For Meteorol 149:1666–1673

Kuzyakov Y, Gavrichkova O (2010) Time lag between photosynthesis and carbon dioxide efflux from soil: a review of mechanisms and controls. Glob Chang Biol 16:3386–3406

Laik R, Kumar K, Das DK, Chaturvedi OP (2009) Labile soil organic matter pools in a calciorthent after 18 years of afforestation by different plantations. Appl Soil Ecol 42:71–78

Lewis SL, Lopez-Gonzalez G, Sonké B, et al. (2009) Increasing carbon storage in intact African tropical forests. Nature 457:1003–1007

Lorenz K, Lal R (2010) Carbon sequestration in forest ecosystems. Springer, New York

Luan JW, Liu SR, Zhu XL, Wang JX, Liu K (2012) Roles of biotic and abiotic variables in determining spatial variation of soil respiration in secondary oak and planted pine forests. Soil Biol Biochem 44:143–150

Luyssaert S, Schulze ED, Börner A, Knohl A, Hessenmöller D, Law BE, Ciais P, Grace J (2008) Old-growth forests as global carbon sinks. Nature 455:213–215

Martin JG, Bolstad PV (2009) Variation of soil respiration at three spatial scales: components within measurements, intra-site variation and patterns on the landscape. Soil Biol Biochem 41:530–543

Moyano FE, Manzoni S, Chenu C (2013) Responses of soil heterotrophic respiration to moisture availability: an exploration of processes and models. Soil Biol Biochem 59:72–85

Ngao J, Epron D, Delpierre N, Bréda N, Granier A, Longdoz B (2012) Spatial variability of soil CO_2 efflux linked to soil parameters and ecosystem characteristics in a temperate beech forest. Agric For Meteorol 154–155:136–146

Odum EP (1969) The strategy of ecosystem development. Science 164:262–270

Ohashi M, Kume T, Yoshifuji N, Kho LK, Nakagawa M, Nakashizuka T (2015) The effects of an induced short-term drought period on the spatial variations in soil respiration measured around emergent trees in a typical Bornean tropical forest, Malaysia. Plant Soil 387:337–349

Prolingheuer N, Scharnagl B, Graf A, Vereecken H, Herbst M (2014) On the spatial variation of soil rhizospheric and heterotrophic respiration in a winter wheat stand. Agric For Meteorol 195:24–31

Robertson GP, Gross KL (1994) Assessing the heterogeneity of below ground resources: quantifying pattern and scale. In: Caldwell MM, Pearcy RW (eds) Exploitation of environmental heterogeneity by plants: ecophysiological processes

above-and belowground. Academic Press, New York, pp. 237–252

Robertson GP, Crum JR, Ellis BG (1993) The spatial variability of soil resources following long-term disturbance. Oecologia 96:451–456

Scott-Denton LE, Rosenstiel TN, Monson RK (2006) Differential controls by climate and substrate over the heterotrophic and rhizospheric components of soil respiration. Glob Chang Biol 12:205–216

Shi BK, Gao WF, Jin GZ (2015) Effects on rhizospheric and heterotrophic respiration of conversion from primary forest to secondary forest and plantations in northeast China. Eur J Soil Biol 66:11–18

Smith KA, Ball T, Conen F, Dobbie KE, Massheder J, Rey A (2003) Exchange of greenhouse gases between soil and atmosphere: interactions of soil physical factors and biological processes. Eur J Soil Sci 54:779–791

Søe ARB, Buchmann N (2005) Spatial and temporal variations in soil respiration in relation to stand structure and soil parameters in an unmanaged beech forest. Tree Physiol 25:1427–1436

Software GD (2004) GS+: geostatistics for the environmental sciences. Gamma Design Software, Plainwell, Michigan

Soil Survey Staff (1999) Soil Taxonomy: A basic system of soil classification for making and interpreting soil surveys. USDA Natural Resources Conservation Service, Washington, D.C

Song W, Chen S, Wu B, Zhu Y, Zhou Y, Lu Q, Lin G (2015) Simulated rain addition modifies diurnal patterns and temperature sensitivities of autotrophic and heterotrophic soil respiration in an arid desert ecosystem. Soil Biol Biochem 82:143–152

State Forestry Administration (SFA) (2005) China forestry yearbook 2005. China Forestry Press, Beijing(in Chinese)

Teixeira DDB, Bicalho ES, Cerri CEP, Panosso AR, Pereira GT, La Scala N (2013) Quantification of uncertainties associated with space-time estimates of short-term soil CO_2 emissions in a sugar cane area. Agric Ecosyst Environ 167:33–37

Wang CK, Yang JY, Zhang QZ (2006) Soil respiration in six temperate forests in China. Glob Chang Biol 12:2103–2114

Wang X, Jiang Y, Jia B, Wang F, Zhou G (2010) Comparison of soil respiration among three temperate forests in changbai mountains, China. Can J For Res 40:788–795

Wang CK, Han Y, Chen JQ, Wang XC, Zhang QZ, Bond-Lamberty B (2013) Seasonality of soil CO_2 efflux in a temperate forest: biophysical effects of snowpack and spring freeze-thaw cycles. Agric For Meteorol 177:83–92

Webster R, Oliver MA (2007) Geostatistics for environmental scientists. John Wiley & Sons Ltd, Chichester

Western AW, Blöschl G (1999) On the spatial scaling of soil moisture. J Hydrol 217:203–224

Xu M, Qi Y (2001) Soil-surface CO_2 efflux and its spatial and temporal variations in a young ponderosa pine plantation in northern California. Glob Chang Biol 7(6):667–677

Yoon TK, Noh NJ, Han S, Lee J, Son Y (2014) Soil moisture effects on leaf litter decomposition and soil carbon dioxide efflux in wetland and upland forests. Soil Sci Soc Am J 78(5):1804–1816

Yuan ZQ, Gazol A, Lin F, Ye J, Shi S, Wang XG, Wang M, Hao ZQ (2013) Soil organic carbon in an old-growth temperate forest: spatial pattern, determinants and bias in its quantification. Geoderma 195:48–55